Cold Nuclear Matter Effects on Quarkonium Production

R. Vogt

Nuclear and Chemical Sciences Division, Lawrence Livermore National Laboratory, Livermore, CA 94551, USA
Physics and Astronomy Department, University of California, Davis, CA 95616, USA

based on:
F. Arleo *et al.*, arXiv:2506.17554, Phys. Rev. C, in press
S. Thapa *et al.*, arXiv:2510.03456, Phys. Rev. D, in press; and in preparation

Figure 1: **This work was performed under the auspices of the U.S. Department of Energy by Lawrence Livermore National Laboratory under Contract DE-AC52-07NA27344 and supported by the U.S. Department of Energy, Office of Science, Office of Nuclear Physics (Nuclear Theory) under contract number DE-SC-0004014 and the HEFTY Collaboration.**

Cold Nuclear Matter Effects: from the LHC to the EIC

F. Arleo *et al.*, (to be published in Phys. Rev C)

CFNS workshop, January 2025: https://indico.cfnssbu.physics.sunysb.edu/event/338/

White paper, arXiv:2506.17454, identified key questions and discussed how to address them

- **Current Data**
- **Leading-Twist nPDF Effects vs. Saturation**
- **Energy Loss in Cold Nuclear Matter**
- **Nuclear Absorption**
- **Other Effects**
  - **Comovers**
  - **Impact Parameter Dependence of nPDF Effects**
  - **Intrinsic Heavy Flavors**
- **Future Experiments**

Some contributions from the paper are now discussed in the context of quarkonium production

New results for quarkonium suppression combining cold and hot QCD effects are also shown

Cold Matter Effects on $p + A$ Quarkonium Production

Perturbative QCD production cross section in $p + A$ collisions

$$\sigma_{pA}^{\rm pQCD}(S, m^2) \; = \; \sum_{i,j=q,\overline{q},g} \int_{4m_Q^2/S}^{1} \frac{d\tau}{\tau} \int d^2b dz d\epsilon \, dx_1 \, dx_2 \, \delta(x_1 x_2 - \tau) \delta(x'_F - x_F - \delta x_F(\epsilon)) \delta(x'_F - x_1 + x_2)$$
$$\times P(\epsilon) \, S_A^{\rm abs}(\vec{r}, z) \, S_{\rm co}(\tau) \, f_i^p(x_1, \mu_F^2, k_T^p) F_i^A(x'_1, \mu_F^2, k_T^A, \vec{b}, z) \, \widehat{\sigma}_{ij}(s, m^2, \mu_F^2, \mu_R^2)$$

Survival probability for absorption of a (proto)charmonium state in nuclear matter

$$S_A^{\rm abs}(b, z) = \exp \left\{ - \int_z^\infty dz' \rho_A(b, z') \sigma_{\rm abs}(z - z') \right\}$$

$S^{\rm co}$ **is the survival probability for quarkonium interactions with comovers**

$P(\epsilon)$ **is energy loss probability that modifies the** x_F **of the produced** J/ψ **state;** k_T **broadening can be combined with energy loss**

Nuclear parton densities, including centrality dependence

$$F_i^A(x, Q^2, \vec{b}, z) = \rho_A(s) S^i(A, x, Q^2, k_T, \vec{b}, z) f_i^p(x, Q^2) \; ; \quad s = \sqrt{b^2 + z^2} \; ; \quad \rho_A(s) = \rho_0 \frac{1 + \omega(s/R_A)^2}{1 + \exp[(s - R_A)/d]}$$

S^i **is nPDF effect on parton** i**; no nuclear modification,** $S^i(A, x, Q^2, \vec{r}, z) \equiv 1$

Intrinsic heavy flavor production is added to the pQCD cross section, calculated to NLO

$$\sigma_{pA}^{\rm tot} \; = \; \sigma_{pA}^{\rm pQCD} + \sigma_{pA}^{\rm iQ}$$

Nuclear PDF Effects vs. Saturation

.

J/ψ A dependence: nPDF effects are insufficient

If nuclear PDF modifications are sufficient to explain J/ψ data, then the results should be independent of $\sqrt{s_{NN}}$ and depend only on x_2

Left hand side shows J/ψ data from fixed-target energies to the LHC. The x_2 range is wide and results are very different, with experiments that reach large x_F showing the strongest modification

Right hand side shows the EPPS16 gluon ratio for W/Be compared to the E866 results from $\sqrt{s_{NN}} = 38.7$ GeV. The EPPS16 results lie consistently above the data.

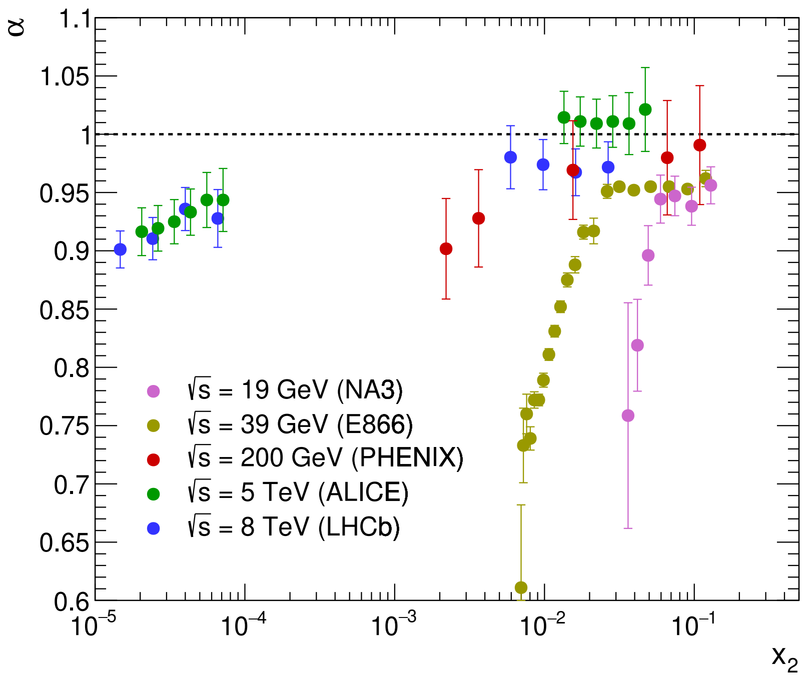

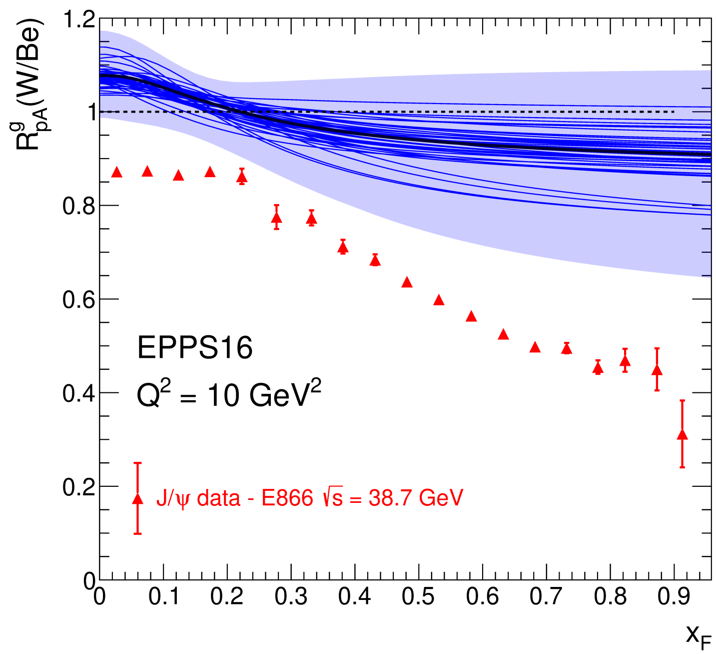

Shadowing vs. Saturation: x and Q^2 range

(Left) DIS and Drell-Yan data cover an x and Q^2 range that does not yet reach into the saturation regime. The EIC kinematic reach will be greater and reach higher Q^2, putting the saturation regime within reach for heavy nuclei, although not penetrating far into it.

(Right) EPPS21 nPDF global analysis covered wider range of hadron and gauge boson production

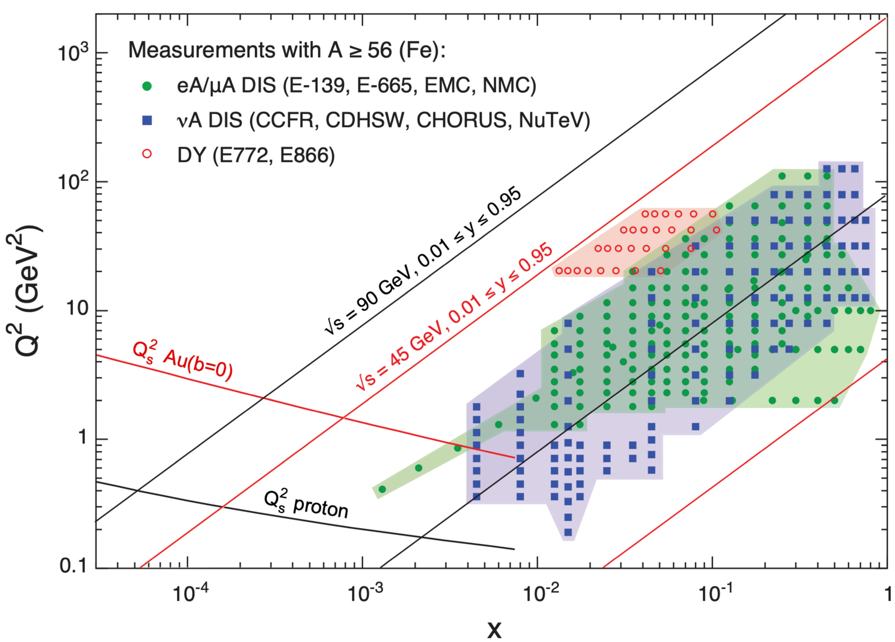

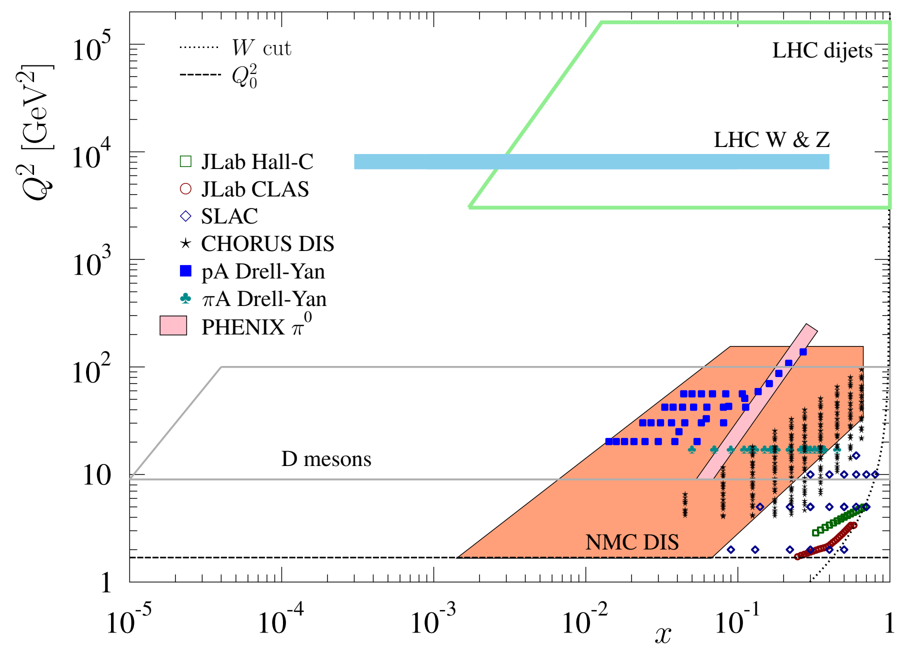

Shadowing vs. Saturation: Observables

1. **Structure function measurements in DIS – CGC and leading-twist shadowing follow different trajectories in the (x, Q^2) plane due to differences in the underlying QCD dynamics. The differences between the two types of evolution are larger for the longitudinal structure function F_L and become larger for a heavy nucleus than in a proton.**

2. **Single particle and correlated pair production in $e + A$ and $p + A$**

   - **Two-particle azimuthal correlations – disappearance of the peak at $180°$ as a function of azimuthal angle in the CGC. Complications: NLO correlations already decorrelate the peak and momentum broadening can remove it (CGC effects also include suppression as well as broadening, different from NLO DGLAP; heavy flavor correlations may be most relevant**
   - **Single-inclusive hadron production in $p + A$ – CGC and nPDF calculations predict different slopes of R_{pA} as a function of y and p_T; limited by typically large nPDF uncertainties**
   - **Single inclusive hadron/jet production in $e + A$ – single inclusive DIS (SIDIS) can probe saturated sea quark distributions for $p_T \sim Q_s \ll Q$; fragmentation can be a complication that can be removed by studying single-inclusive jet production**

3. **Diffractive vector meson production in $\gamma + A$ – UPCs probe low x gluon distributions, particularly for J/ψ production**

Energy Loss

•

Energy loss in medium

Based on the relative size of the formation time of a soft radiated gluon compared to the medium it travels through, the matter the gluon scatters with can be seen as incoherent scattering centers (Bethe-Heitler); partially coherent, with a group of scattering centers acts like a single radiator (LPM regime); full coherent (FCEL) where all scattering centers acts like a radiation source; and Bertsch-Gunion regime (BG-like) where initial state interactions can partially cancel radiation effects

	ΔE	Observables	Systems	Facilities
Initial state LPM	$\hat{q}\,L^2\,\ln E$	Drell-Yan	$h + A$	E906, COMPASS
Final state LPM	$\hat{q}\,L^2\,\ln E$	h, jets	$e + A$	CLAS, HERMES, EIC
FCEL	$(\hat{q}\,L)^{1/2}\,(E/M_T)$	h, jets	$h + A$	SPS, FNAL, RHIC, LHC
BG-like	$f(\hat{q}\,L)L\,E$	high x_F Drell-Yan, h, jets	$h + A$	FNAL, RHIC, LHC

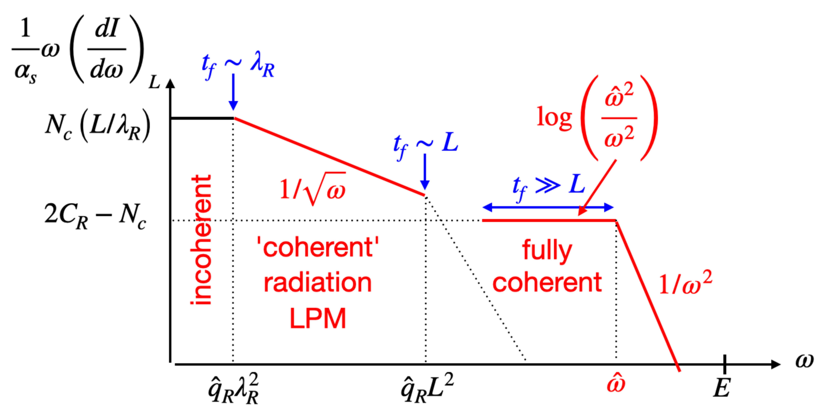

Transport Coefficient $\hat{q}$

Strength of induced gluon radiation governed by transport coefficient $\hat{q}$, related to the gluon distribution evaluated at the momentum scale $Q^2 \sim \Delta p_T^2$.

$$\hat{q} \equiv \frac{\tilde{\mu}^2}{\lambda} = \frac{4\pi^2 \alpha_s C_R}{N_c^2 - 1} \rho\, x g\left(x, Q^2\right)$$

$\hat{q}$ can be determined from analyses of transverse momentum broadening, $\Delta p_T^2 = \left\langle p_T^2 \right\rangle_{hA} - \left\langle p_T^2 \right\rangle_{hp}$, related to multiple parton scattering

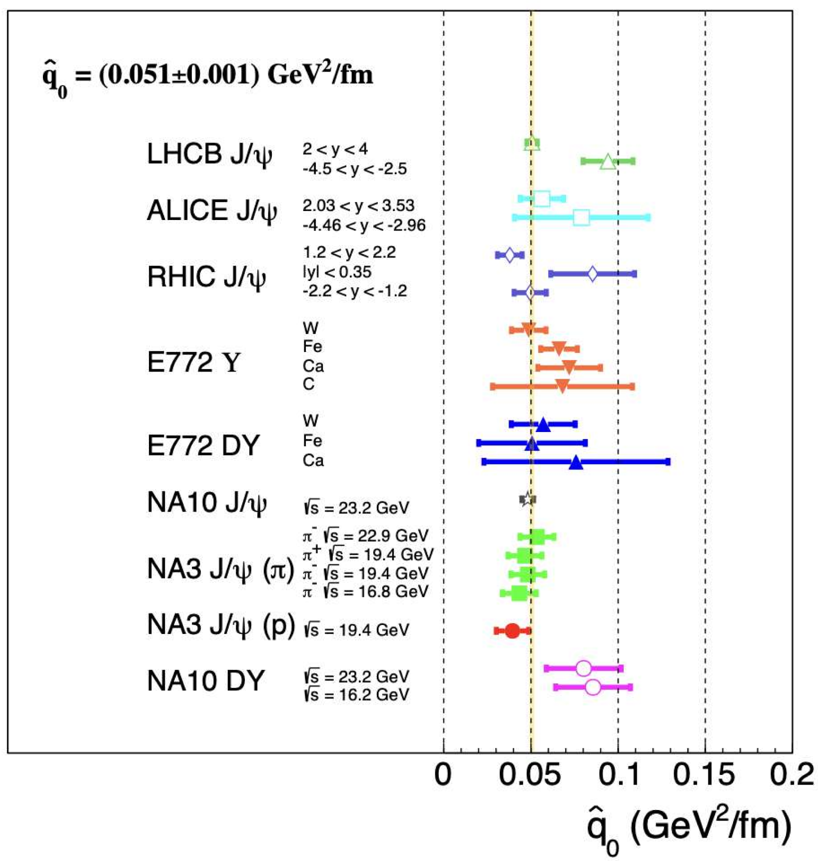

Using J/ψ Data to Pin down Nuclear Gluon PDF

The nPDF uncertainty on the low x gluon distribution can be large just based on DIS and DY data

The J/ψ is predominantly produced by gluons but is subject to other effects

Including J/ψ data can significantly reduce the uncertainties but the amount of low x shadowing depends on whether or not energy loss is taken into account

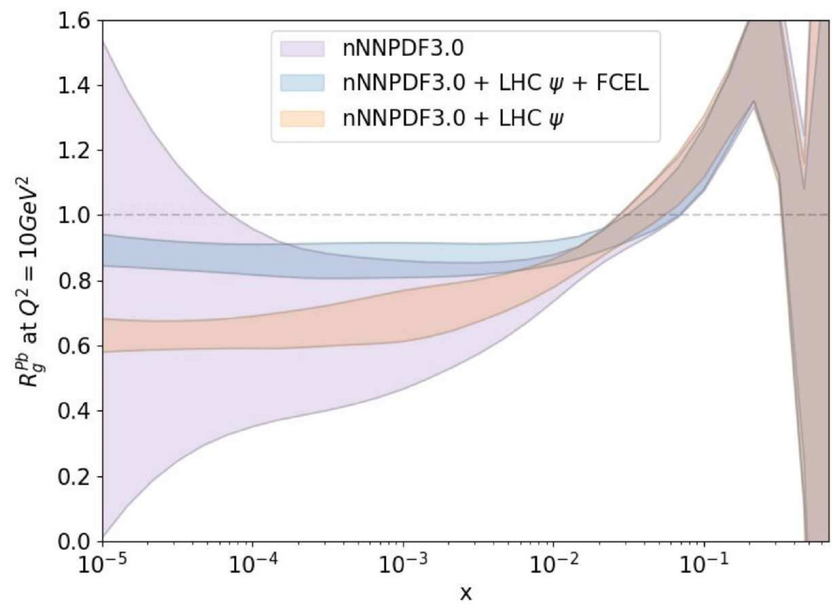

Energy Loss: Observables

1. **Drell-Yan at high x_F – well suited for studies of LPM energy loss**
2. **J/ψ production in $e+A$ and $p+A$ – FCEL depends on the color structure of the partonic process and is thus not universal; comparison of $e+A$ and $p+A$ J/ψ production could test this non-universality**

$$\begin{aligned} R_{eA}^{J/\psi}(x) &\simeq R_{eA}^{\mathbf{nPDF}}(x) \approx R_g^A(x); \\ R_{pA}^{J/\psi}(y, x_2) &\simeq R_{pA}^{\mathbf{nPDF+FCEL}}(y, x_2) \\ &\approx R_g^{\mathbf{A}}(x_2) \times R_{pA}^{\mathbf{FCEL}}(y, x_2)\,. \end{aligned}$$

3. **Direct and resolved photoproduction of forward jets and hadrons – resolved photoproduction would be sensitive to FCEL while direct photoproduction is not**
4. **$R_{pA}^{J/\psi}/R_{pA}^{\mathrm{DY}}$ at forward rapidity or large x_F – this ratio should be above unity for nPDF effects alone but smaller than unity for FCEL**
5. **$R_{pA}^{J/\psi}/R_{pA}^{\Upsilon}$ – FCEL is mass dependent, scaling like $1/m_T$, while nPDF evolution reduces the mass dependence of this effect**
6. **p_T broadening – useful for extracting $\hat{q}$ and constraining energy loss in Drell-Yan, quarkonium production, or SIDIS**
7. **Light hadrons and heavy flavors at large x_F – Bertsch-Gunion type energy loss can suppress energetic final-states at large x_F**

Absorption and Comovers: Final-State Effects

.

Absorption by Nucleons

.

Is Absorption Important for J/ψ Production?

Different methods used to extract an absorption cross section reach different conclusions about the size of $\sigma_{\rm abs}$

The absorption cross section is related to the production model (singlet, octet, or some combination) and to whether or not other CNM effects are included

Originally, absorption was a ‘catch all’ to cover all effects with a single, kinematics dependent parameter α, $\sigma_{pA} = \sigma_{pp} A^\alpha$

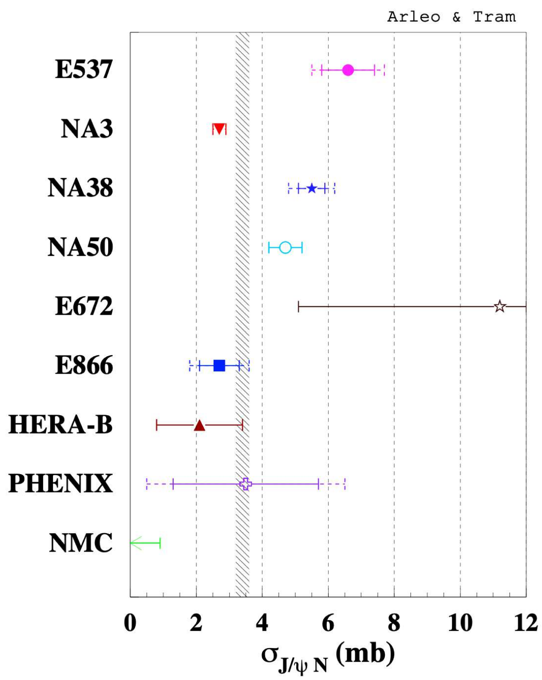

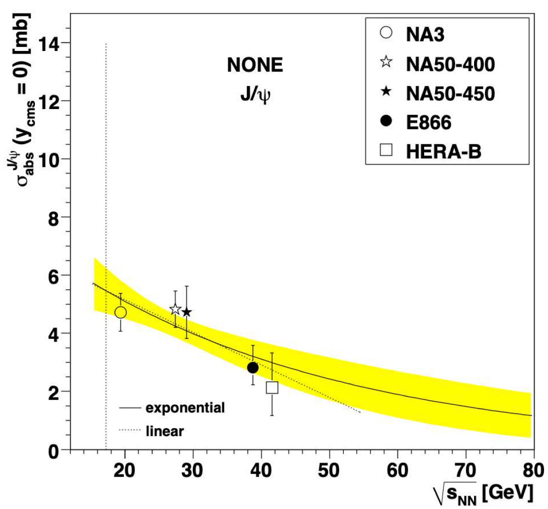

Interplay of nPDF Effects and Absorption

Depending on x values probed, shadowing can enhance or reduce absorption cross section needed to describe data

Absorption alone always gives less than linear A dependence ($\alpha < 1$)

For SPS energies, $17.3 \leq \sqrt{S} \leq 29$ GeV, rapidity range covered is in EMC and antishadowing region, $\alpha > 1$ with no absorption

Adding shadowing to absorption in the SPS energy region requires a larger absorption cross section is needed to maintain agreement with data

For $\sqrt{S} \geq 38$ GeV, x in shadowing regime, thus $\alpha < 1$ with shadowing alone in forward region, reducing needed absorption cross section to $\sigma_{\rm abs} \sim 0$ at the LHC

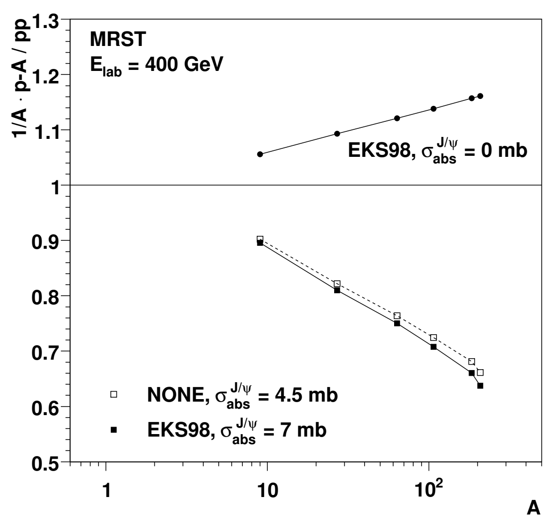

Figure 2: **(Left) Illustration of the interplay between shadowing and absorption. [C. Lourenco, H. K. Woehri and RV, JHEP 0902 (2009) 014.]**

$\sigma_{\rm abs}$ Grows with Time $c\bar{c}$ Spends Traversing Nucleus

Mid- and backward rapidity J/ψ at $\sqrt{s_{NN}} = 200$ GeV (longer $\tau = L/\gamma$) dominated by conversion of color octet $c\bar{c}$ pair to color singlet J/ψ by gluon emission

$$\sigma_{\rm abs}(\tau) = \sigma_1 \left(\frac{\sqrt{s}}{10\ GeV}\right)^{0.4} \left(\frac{r_{c\bar{c}}(\tau)}{r_{{\rm J}/\psi}}\right)^2 \qquad r_{c\bar{c}}(\tau) = r_0 + v_{c\bar{c}}\tau \text{ for } r_{c\bar{c}}(\tau) < r_\psi$$

Difference at forward rapidity (shorter τ) where conversion occurs outside target

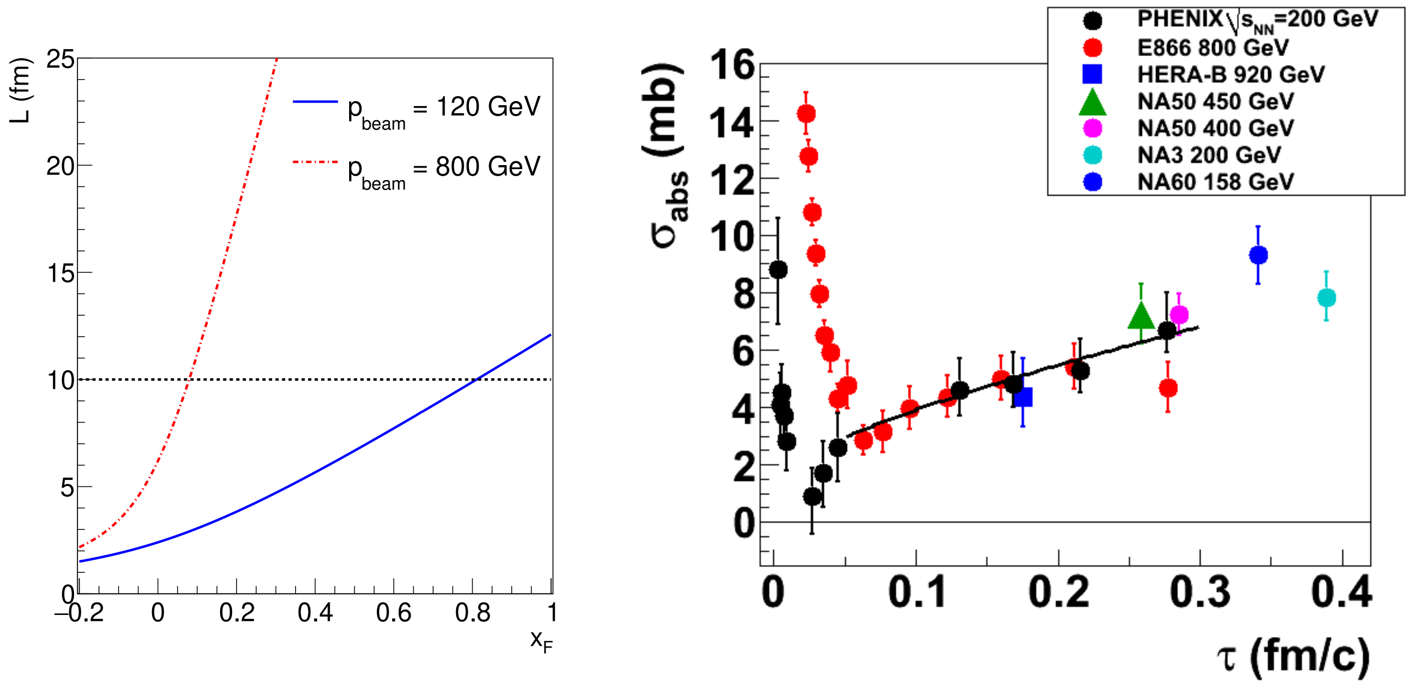

Figure 3: The effective $c\bar{c}$ breakup cross section as a function of the proper time spent in the nucleus, τ. The values were extracted from PHENIX $\sqrt{s_{NN}} = 200$ GeV d+Au data after correction for shadowing using EPS09 and from fixed-target p+A data measured by E866 at 800 GeV, by HERA-B at 920 GeV, by NA50 at 450 GeV and 400 GeV, by NA3 at 200 GeV, and by NA60 at 158 GeV. In all fixed-target cases, the EKS98 parameterization was used. The curve is calculated based on octet-to-singlet conversion inside the nucleus. [D. McGlinchey, A. D. Frawley and RV, Phys. Rev. C **87** (2013) 054910.]

Comover Interaction Model

.

Comover Interaction Model, Ferriero *et al.*

Comover interaction rate

$$\Gamma^{\mathcal{Q}}(T) = \int_{E_{\rm thr}^{\mathcal{Q}}}^{\infty} dE^{\rm co}\, \sigma_{\rm geo}^{\mathcal{Q}} \left(1 - \frac{E_{\rm thr}^{\mathcal{Q}}}{E^{\rm co}}\right)^n \frac{\rho^{\rm co}}{e^{E^{\rm co}/T_{\rm eff}} - 1} \quad (1)$$

$E_{\rm thr}^Q = M_Q + m_{\rm co} - 2M_H$ **where** $Q = c$ **or** b**,** $H = D$ **or** B**,** $E^{\rm co} = \sqrt{p^2 + m_{\rm co}^2}$ **with** $m_{\rm co} = 0$ **for gluons and 140 MeV for pions;** ρ^0 **is the transverse density of comovers, proportional to the multiplicities;** $\sigma_{\rm geo}^0 \simeq \pi r_Q^2$**; the power** n **is between 0.5 and 2 and** $T_{\rm eff} \simeq 200 - 300$ **MeV**

Dissociation of quarkonium by comover interactions as a function of time

$$\tau \frac{\mathbf{d}\rho^{\mathcal{Q}}}{\mathbf{d}\tau}\,(b,s,y) \;=\; -\sigma^{\rm co-\mathcal{Q}}\, \rho^{\rm co}(b,s,y)\, \rho^{\mathcal{Q}}(b,s,y)\;, \quad (2)$$

$\sigma^{\rm co-Q}$ **is the energy-averaged quarkonium-comover interaction cross section**

The densities of comovers and quarkonium are $\rho^{\rm co}$ **and** ρ^Q **respectively**

Integrating over time τ **from** τ_i **to** τ_f **gives the survival probability**

$$S_{\mathcal{Q}}^{\rm co}(b,s,y) \;=\; \exp\left\{ -\, \sigma^{\rm co-\mathcal{Q}}\, \rho^{\rm co}(b,s,y)\, \ln\left(\rho^{\rm co}(b,s,y)/\rho_{pp}(y)\right)\right\} \quad (3)$$

Shadowing is included but other cold matter effects are not

The different sizes of $\sigma^{\rm co-Q}$ **for** $Q = J/\psi$ **and** ψ**(2S) result in stronger comover dissociation for** ψ' **than** J/ψ

It has been shown that the A **dependence of comover interactions and nucleon absorption are effectively the same (Gavin and Vogt)**

Comover Effects on Charmonium at the LHC

$\sigma^{\mathrm{co}-Q}$ **was fixed to fits to low-energy experimental data to be** $\sigma^{\mathrm{co}-J/\psi} = 0.65$ **mb for the** J/ψ **and** $\sigma^{\mathrm{co}-\psi(2\mathrm{S})} = 6$ **mb for the** ψ**(2S)**

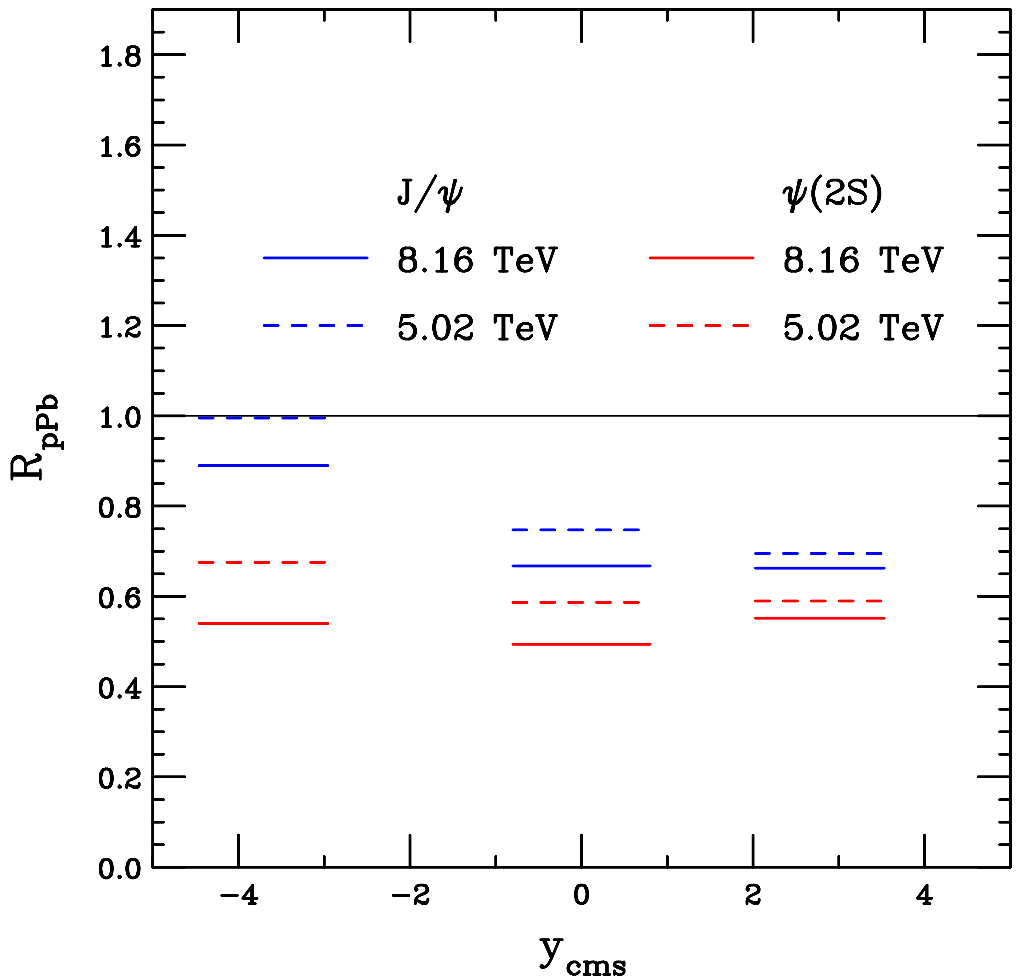

Figure 4: **The rapidity dependence of** J/ψ **and** ψ**(2S) production in the comover interaction model at 5.02 and 8.16 TeV. The EPS09 LO shadowing parameterization is also included. From Elena Ferreiro, in NPA 972 (2018) 18, arXiv:1707.09973 [hep-ph].**

Absorption and Comovers: Observables

1. **Double ratios of quarkonium states, $R^{Q\overline{Q}_i}/R^{Q\overline{Q}_j}$ – this ratio should be independent of nPDF and energy loss effects and so could isolate absorption effects for $t_{\rm form} \leq L$ where there are few comovers**

2. **Double ratios of quarkonium states, $R^{Q\overline{Q}_i}/R^{Q\overline{Q}_j}$ – in high energy collisions, $t_{\rm form} \gg L$ and absorption is negligible, this double ratio could then isolate comover effects; comparison between the double ratios for quarkonium and open heavy flavor mesons could further separate comovers from other effects**

3. **$R^{J/\psi}$ vs. R^{χ_c} – differences in the color state at production could result in different absorption cross sections**

4. **Hadron production in SIDIS in $e+p$ vs. $e+A$ – absorption effects can be isolated in regions were energy loss and nPDF effects are small**

Impact Parameter Dependent nPDF Effects

.

Impact Parameter Dependent Shadowing

.

Impact parameter dependence of shadowing first proposed in Phys. Rev. C 56, 2726 (1997)

Two parameterizations chosen, one with shadowing proportional to the nuclear density and the other proportional to the nuclear thickness at the collision point
Both are normalized such that $(1/A)\int d^2b dz \rho(s) S^i(A,x,Q^2,\vec{b},z) = S^i(A,x,Q^2)$

$$S^i_{\rm WS} = S^8(A,x,Q^2,\vec{b},z) = 1 + N_{\rm WS}(S^8(A,x,Q^2)-1)\frac{\rho(\vec{b},z)}{\rho_0}$$

$$S^i_{\rm R}(A,x,Q^2,\vec{b},z) = \begin{cases} 1 + N_{\rm R}(S^i(A,x,Q^2)-1)\sqrt{1-(b/R_A)^2} & b \leq R_A \\ 1 & b > R_A \end{cases} , \qquad (4)$$

McGlinchey *et al.* **tried two forms for the impact parameter dependence after these original forms proved too weak for PHENIX d+Au data:**
EPS09s parameterization keeps powers $n = 1 \cdots 4$ **for** A**-independent coefficients**

$$S^i(A,x,Q^2,\vec{b},z) = 1 - (1 - S^i(A,x,Q^2)\,)\left(\frac{T^n_A(b)}{a(n)}\right)$$

Impact parameter dependence assumed to be a step function with radius R **and diffuseness** d **kept as free parameters**

$$S^i(A,x,Q^2,\vec{b},z) = 1 - \left(\frac{1 - S^i(A,x,Q^2)}{a(R,d)(1+\exp((b-R)/d))}\right)$$

Centrality Dependence of CNM on J/ψ in d+Au Collisions

$$\begin{aligned}
\text{Path Length Dependence}\;\; S^i_\rho(A,x,Q^2,\vec{r},z) &= 1 + N_\rho(S^i(A,x,Q^2)-1)(T_A(\vec{r})/T_A(0))^n \\
\text{Step function Behavior}\;\; S^i_\theta(A,x,Q^2,r_T) &= 1 - (\frac{1-S^i(A,x,Q^2)}{a(R,d)})/(1+\exp(r_T-R)/d))\ ,
\end{aligned}$$

Shadowing appears to be concentrated in core of Au nucleus

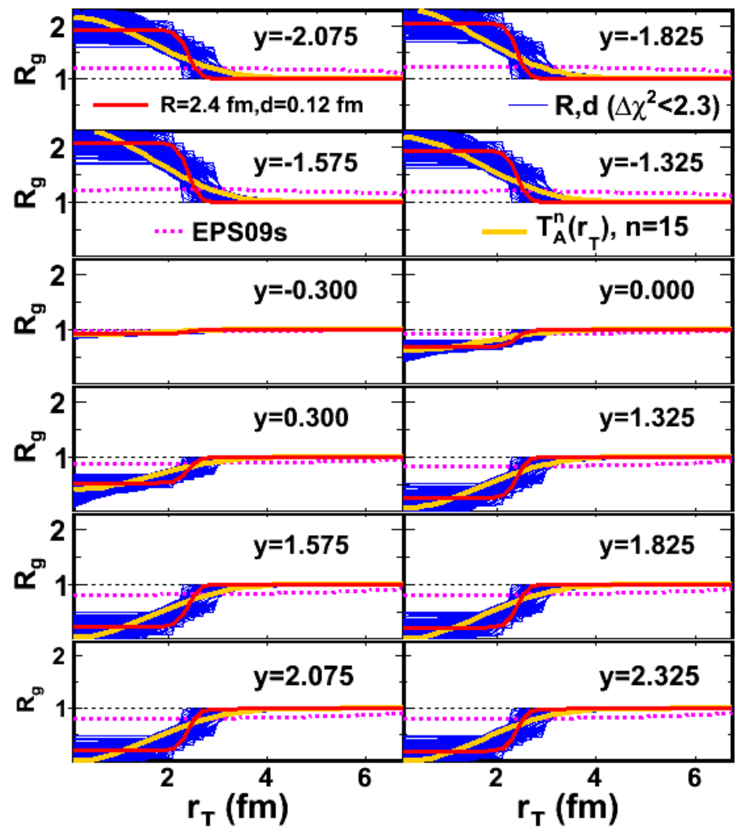

Figure 5: **Transverse radius dependence of gluon shadowing ratio R_g (based on EPS09 NLO) for the PHENIX d+Au rapidity bins. The results compare b-dependence based on path length through the nucleus, $T_A(b)$, and a sharp surface with radius and diffuseness parameters.**

Intrinsic Heavy Flavor Production

.

What are Intrinsic Heavy Flavors?

Proton wavefunction can be expanded as sum over complete basis of quark and gluon states: $|\Psi_p\rangle = \sum_m |m\rangle \, \psi_{m/p}(x_i, k_{T,i}, \lambda_i)$

$|m\rangle$ **are color singlet state fluctuations into Fock components** $|uud\rangle$**,** $|uudg\rangle \cdots |uudc\overline{c}\rangle$

The intrinsic Q **fluctuations can be freed by a soft interaction if the system is probed during the time** $\Delta t = 2p_{\rm lab}/M^2_{c\overline{c}}$ **that the fluctuations exist**

Dominant Fock state configurations have minimal invariant mass, $M^2 = \sum_i m^2_{T,i}/x_i$**, where** $m^2_{T,i} = k^2_{T,i} + m^2_i$ **is the squared transverse mass of parton** i **in the state; corresponds to configurations with equal rapidity constituents**

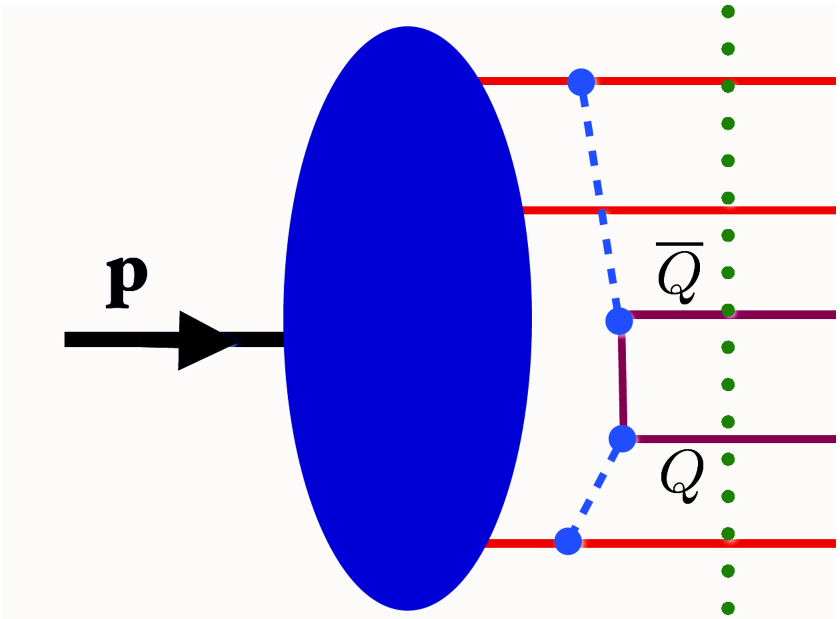

Production by Intrinsic Heavy Quarks

Probability distribution of five-particle Fock state of the proton:

$$dP_{\mathrm{iQ}\,5} = P^0_{\mathrm{iQ}\,5} N_5 \int dx_1 \cdots dx_5 \int dk_{x\,1} \cdots dk_{x\,5} \int dk_{y\,1} \cdots dk_{y\,5} \frac{\delta(1 - \sum_{i=1}^5 x_i)\delta(\sum_{i=1}^5 k_{x\,i})\delta(\sum_{i=1}^5 k_{y\,i})}{(m_p^2 - \sum_{i=1}^5 (\widehat{m}_i^2/x_i))^2}$$

$i = 1, 2, 3$ **are** u, u, d **light quarks, 4 and 5 are** Q **and** $\overline{Q}$**,** N_t **normalizes the probability to unity and** P^0_{ic} **scales the normalized probability to the assumed intrinsic charm content: 0.1%, 0.31% and 1% are used to represent the range of probabilities assumed previously (based on original Brodsky** *et al.* **model, intrinsic bottom content would be approximately an order of magnitude smaller**

The intrinsic charm cross section is determined from soft interaction scale breaking coherence of the Fock state, $\mu^2 = 0.1$ **GeV**^{2}

$$\sigma^{\mathrm{ic}}_{pp} = P_{\mathrm{ic}\,5}\sigma^{\mathrm{in}}_{pN}\frac{\mu^2}{4\widehat{m}_c^2}$$

The cross sections from intrinsic charm are then obtained by multiplying by the normalization factor for the CEM to the J/ψ

$$\sigma^{\mathrm{ic}}_{pp}(J/\psi) = F_C \sigma^{\mathrm{ic}}_{pp} \quad \sigma^{\mathrm{ic}}_{pA} = \sigma^{\mathrm{ic}}_{pp} A^\beta \quad , \beta = 0.71 \ \ (\mathrm{NA3})$$

Other assumptions of intrinsic charm distributions in the nucleon are the meson cloud model ($c(x) \neq \overline{c}(x)$**) and a sea-like distribution (**$c(x) = \overline{c}(x) \propto \overline{d}(x) + \overline{u}(x)$**)**

Recent and Forthcoming Fixed-Target Experiments Ideal for IC Studies

Many previous experiments studied J/ψ production off nuclear targets at proton beam energies from 158 to 920 GeV, several used to get a baseline for $A+A$ collisions; those that covered large x_F saw a larger suppression of production off nuclear targets at higher x_F

SeaQuest: Took data with a 120 GeV proton beam on p, d, C, Fe, and W targets, covered forward region, $0.4 < x_F < 0.95$ and $p_T < 2.3$ GeV; J/ψ data not published yet but should report nuclear suppression factor, $pA/p\mathrm{d}$

SMOG: Gas jet target in LHCb, J/ψ and D^0 measured at backward rapidity in the fixed-target center of mass, data so far at: $p + \mathrm{Ne}$ at $\sqrt{s_{NN}} = 68.5$ GeV; $p + \mathrm{He}$ at $\sqrt{s_{NN}} = 86.6$ GeV; and $p + \mathrm{Ar}$ at $\sqrt{s_{NN}} = 110.4$ GeV

NA60+: proton beams at $p_{\rm lab} = 40$, 80, and 120 GeV, nuclear targets from Be to Pb

Calculations and comparison to data in the following from R. Vogt, arXiv:2101.02858, Phys. Rev. C 103, 035204 (2021); arXiv:2207.04347, Phys. Rev. C 106, 025201 (2022); arXiv:2304.03451, Phys. Rev. C 108, 015201 (2023)

SMOG J/ψ Results Compared to Calculations

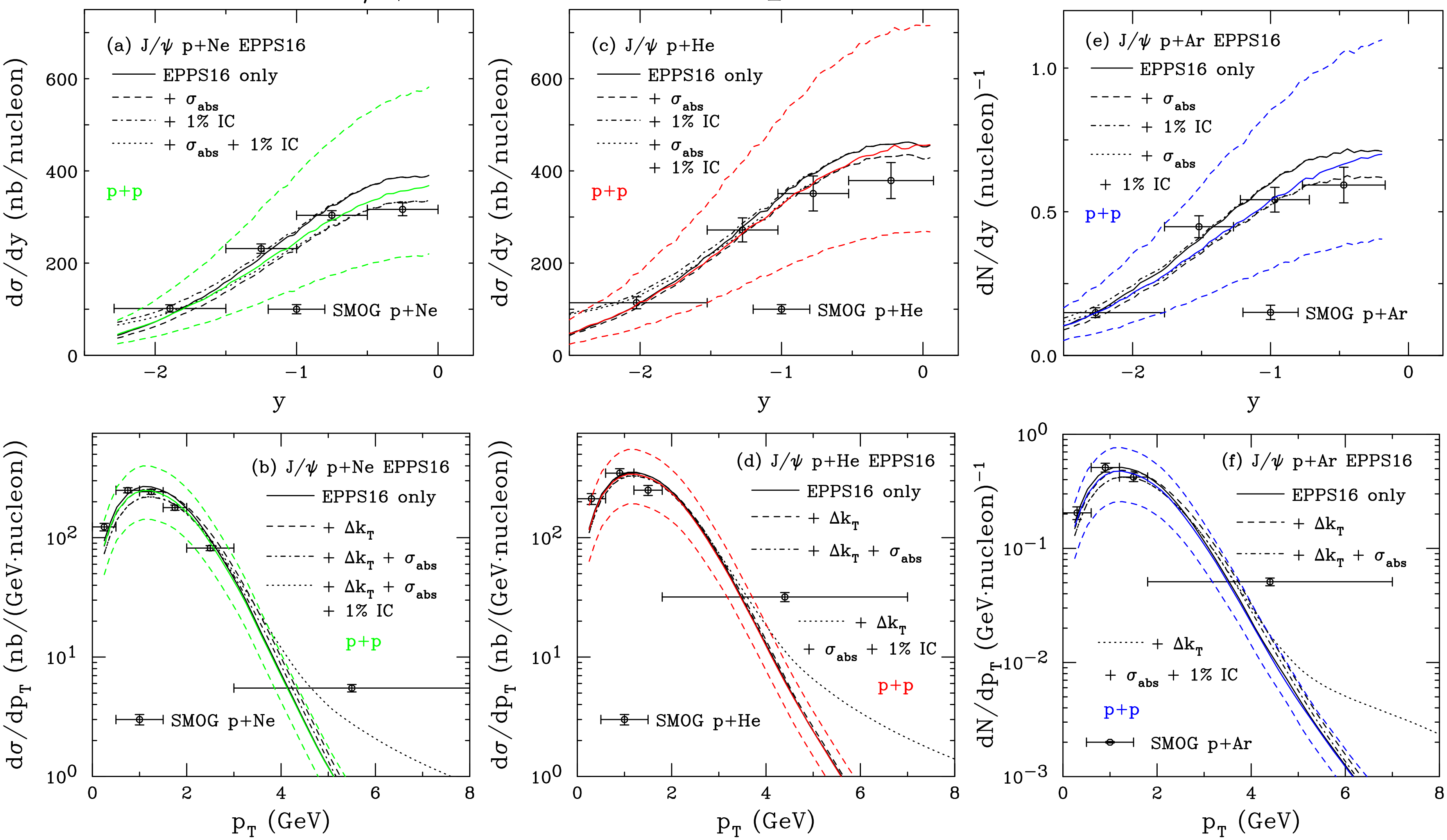

Figure 6: The J/ψ cross section as a function of y in (a), (c), (e) and p_T in (b), (d), (f) for $p+$Ne ($\sqrt{s_{NN}} = 68.5$ GeV) in (a) and (b); $p+$He ($\sqrt{s_{NN}} = 86.6$ GeV) in (c) and (d); and $p+$Ar ($\sqrt{s_{NN}} = 110.4$ GeV) in (e) and (f). The black curves are the $p+A$ calculations. The colored curves (solid and dashed) show the CEM $p+p$ calculations (no IC). The $p+A$ rapidity distributions are shown for EPPS16 only (solid); EPPS16 with absorption (dashed); EPPS16 and $P^0_{\rm ic\,5} = 1\%$ (dot-dashed); and EPPS16, absorption, and $P^0_{\rm ic\,5} = 1\%$ (dotted). The p_T distributions show EPPS16 only (solid); EPPS16 with k_T kick (dashed); EPPS16, absorption, and k_T kick (dot-dashed); and EPPS16, absorption, k_T kick and $P^0_{\rm ic\,5} = 1\%$ (dotted). The $p+$Ne data are from arXiv:2211.11645; the $p+$He and $p+$Ar data are from PRL **122**, 132002 (2019).

Observables for Centrality Dependent nPDFs and Intrinsic Heavy Flavors

1. **Impact parameter dependence of nPDFs – is the nucleus made up of shadowing hot spots or is shadowing uniform throughout the nucleus? PHENIX d+Au data suggested the former while ALICE data may suggest the latter. The EIC should study $e + A$ DIS as a function of impact parameter/event multiplicity.**
2. **Intrinsic heavy flavors – $e + p$ EIC measurements could be decisive**

Do Hot Matter Effects Play a Role in $p + A$?

.

Bottomonium Suppression by CNM at the LHC

nPDF effects and energy loss are not final-state dependent: no distinction between ground state and excited states

Absorption and comovers can depend on the final state but at the LHC, absorption will not play a significant role, even at (measurable) backward rapidity because the states are produced well outside the target

Comovers may have more impact on excited states but this is smaller for Υ than for J/ψ

Comovers could be either hadrons or partons (Ferreiro)

The effect in $p+A$ would be larger in the backward region where there are more produced particles

The figure below shows nPDF and energy loss effects only

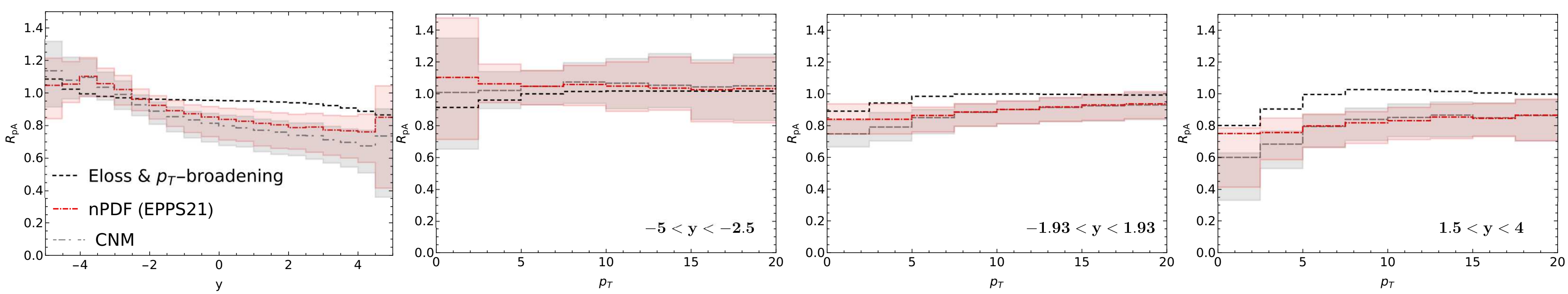

Hot Matter: Open Quantum Systems

NLO pNRQCD open quantum systems approach (PRD 109 (2024) 096016, arXiv:2401.16704 [nucl-th]), labeled KSU-QTraj in figures

- **Quarkonium evolution based on Lindblad equation with dynamics governed by transport coefficients; dissipative and decohering effects encoded in jump operators describing singlet-singlet, singlet-octet and octet-octet transitions, implemented in QTraj code**
- **Differences in suppression for Υ states arises dynamically from state-dependent quantities such as $\langle r^2 \rangle$ and singlet-octet overlaps as well as dependence of the Hamiltonian and width operators on binding energies and level structure**
- **A common medium initialization time $\tau = 0.6$ fm is used for all states**

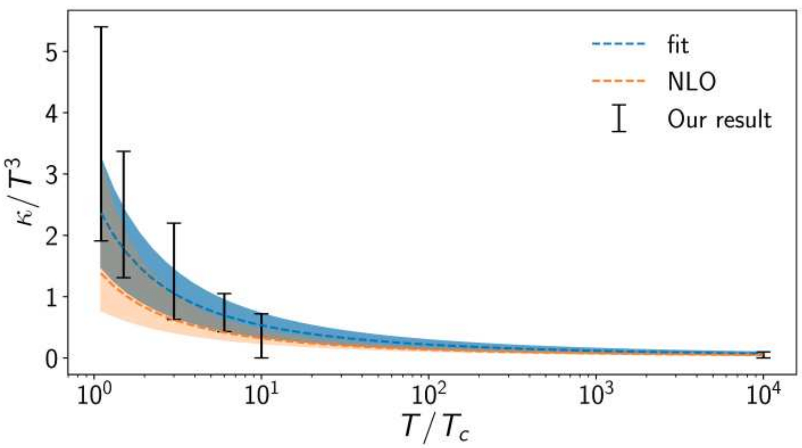

FIG. 13. Temperature dependence of our results compared to the NLO result. The shaded bands include the errors coming from varying the scale by a factor of 2. The blue band also includes the statistical error.

Hot Matter: Semiclassical TAMU Treatments

Rates obtained using two different semiclassical kinetic approaches from the Texas A&M group

- **Quasi-free inelastic scattering and gluo-dissociation employing a perturbative coupling to the medium, labeled TAMU-P in figures**
- **In-medium T-matrix calculations with input potential constrained by lattice QCD calculations of Wilson line correlators, labeled TAMU-NP in figures**
- **Differences in rates and formation times lead to different suppression patterns for Υ states**
- **Regeneration is also considered for TAMU-NP**

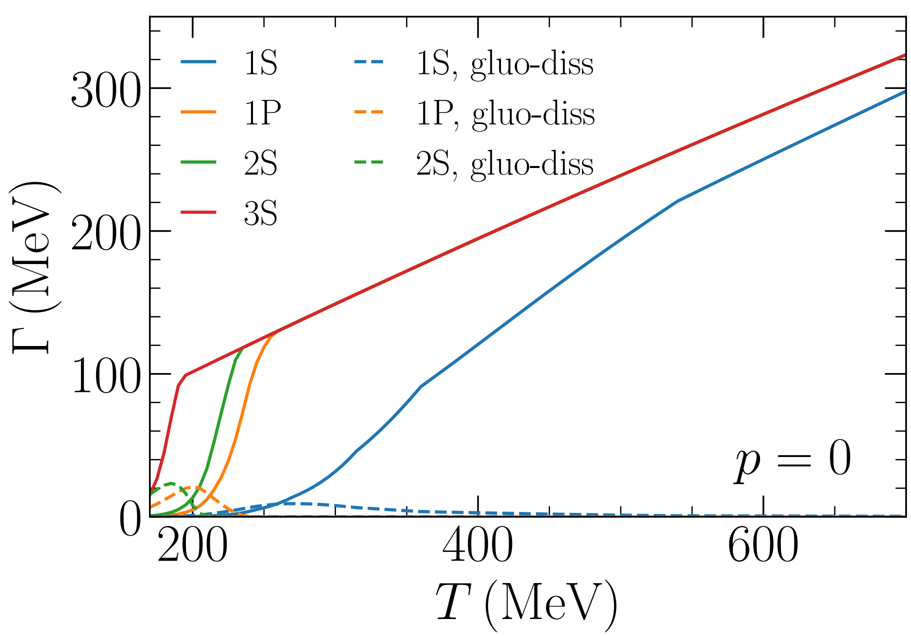

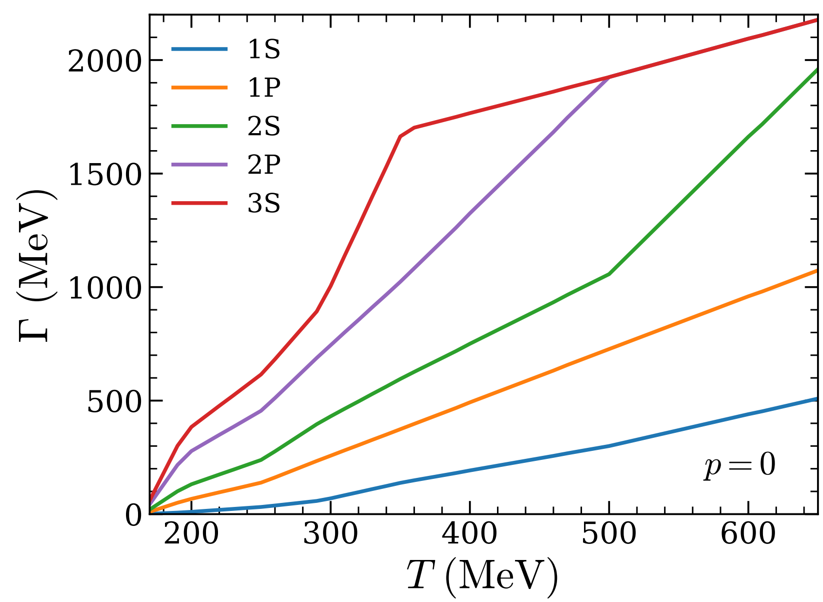

Background Hydrodynamics

Anisotropic nonequilibrium hydrodynamic background calculated using the aHydro3p1 code (arXiv:1807.04337), bottomonium states start interacting with matter after 0.6 fm for open quantum systems (QTraj approach) and after formation time, $\propto 1/E_B$ in TAMU approaches

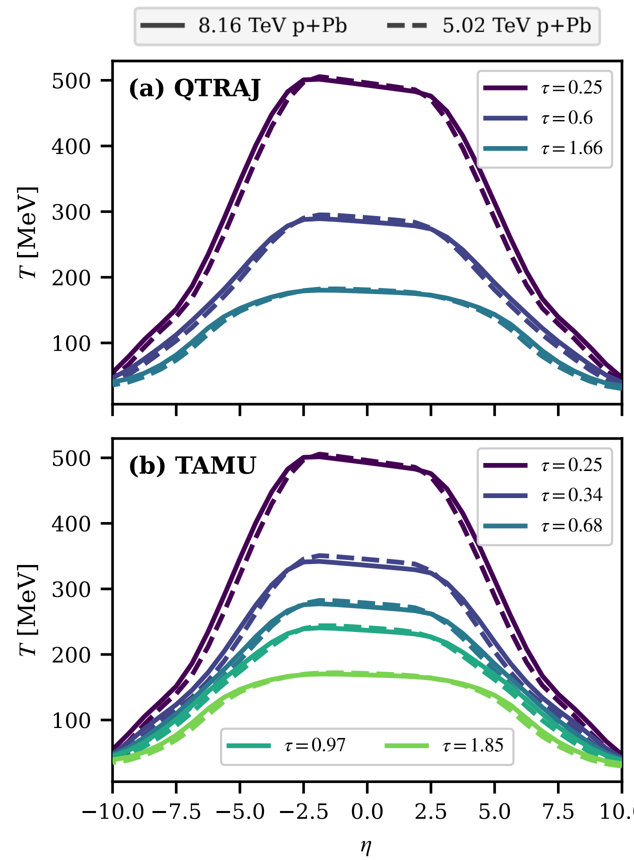

Hot Matter Effects Alone

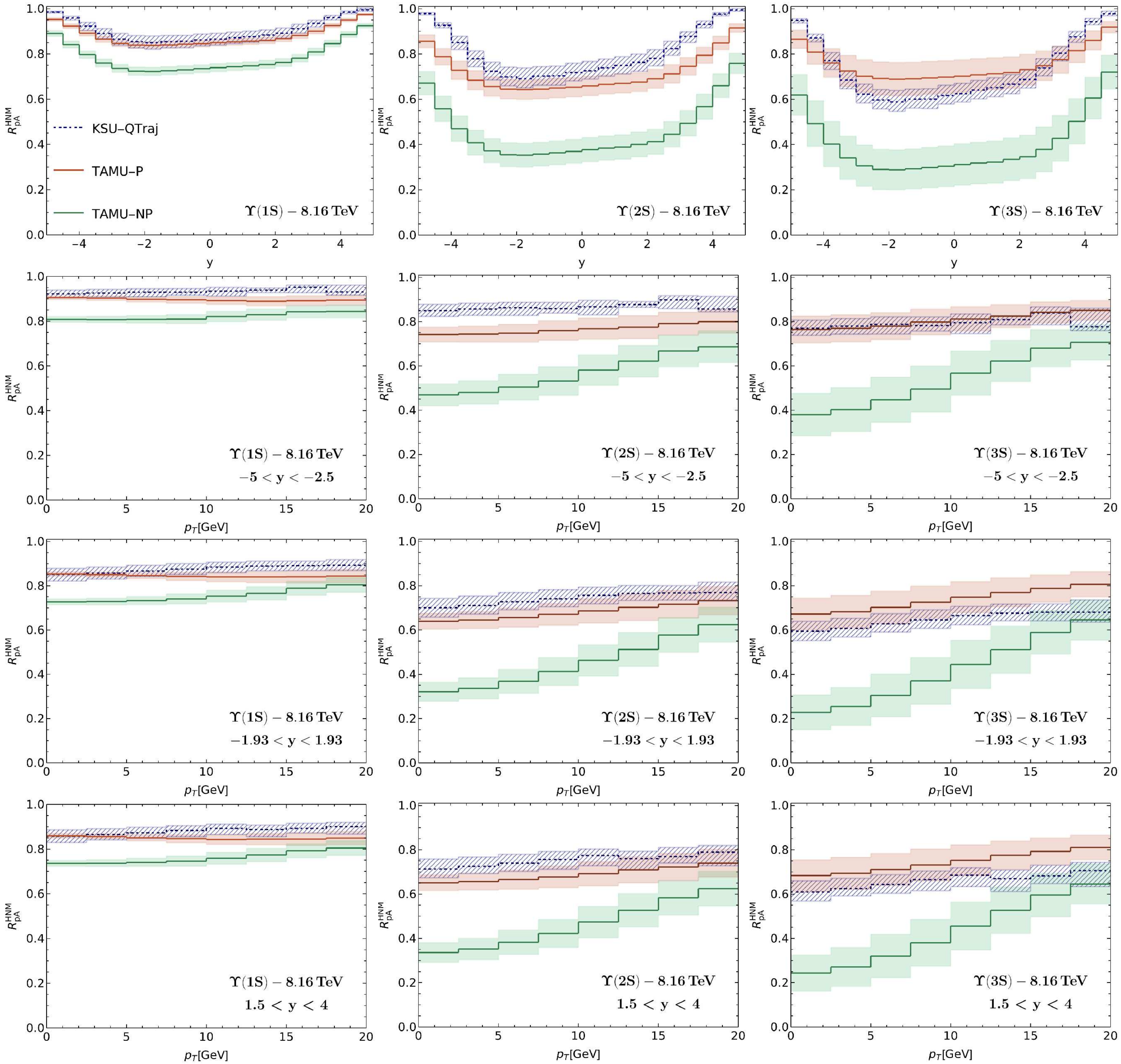

Combined Suppression, without and with Regeneration

Rapidity dependence with both CNM and hot matter effects shown

TAMU-NP rates significantly increase suppression, adding regeneration helps bring the results closer to data

Smaller TAMU-P rates would also reduce regeneration; QTraj results include regeneration when transitions are taken into account

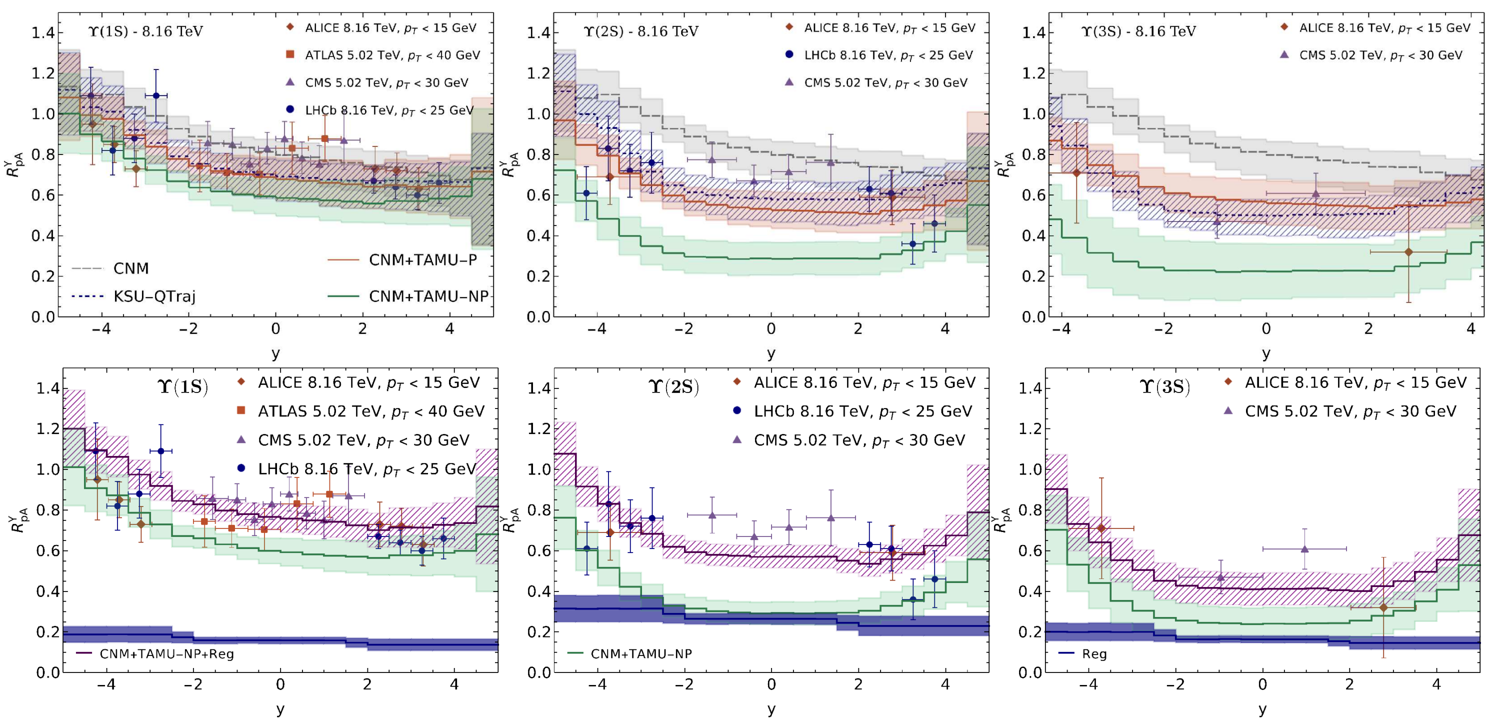

Extending Calculations to Charmonium

Calculations will treat both the LHC and RHIC

Only cold matter effects are included so far, the calculation is still in progress.

Impact parameter dependent shadowing is included; uncertainties introduced for energy loss and k_T broadening

Same hydro background is used but centrality dependence needs to adopted

Absorption will be included for RHIC energies

Only TAMU rates will be used here: no open quantum systems calculation exists for charmonium

Centrality Dependent CNM Effects vs y

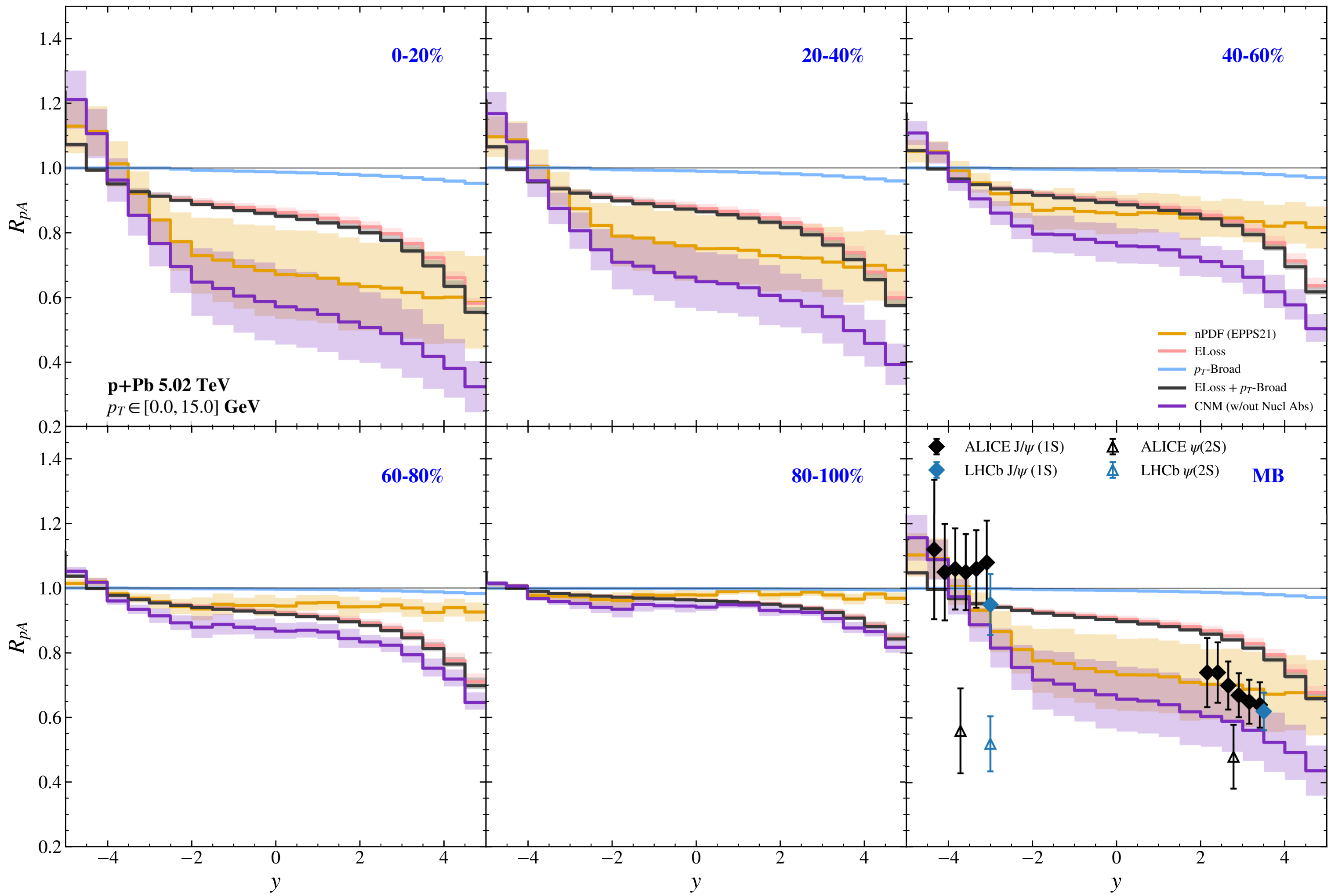

Centrality Dependent CNM Effects vs p_T in 3 y Bins

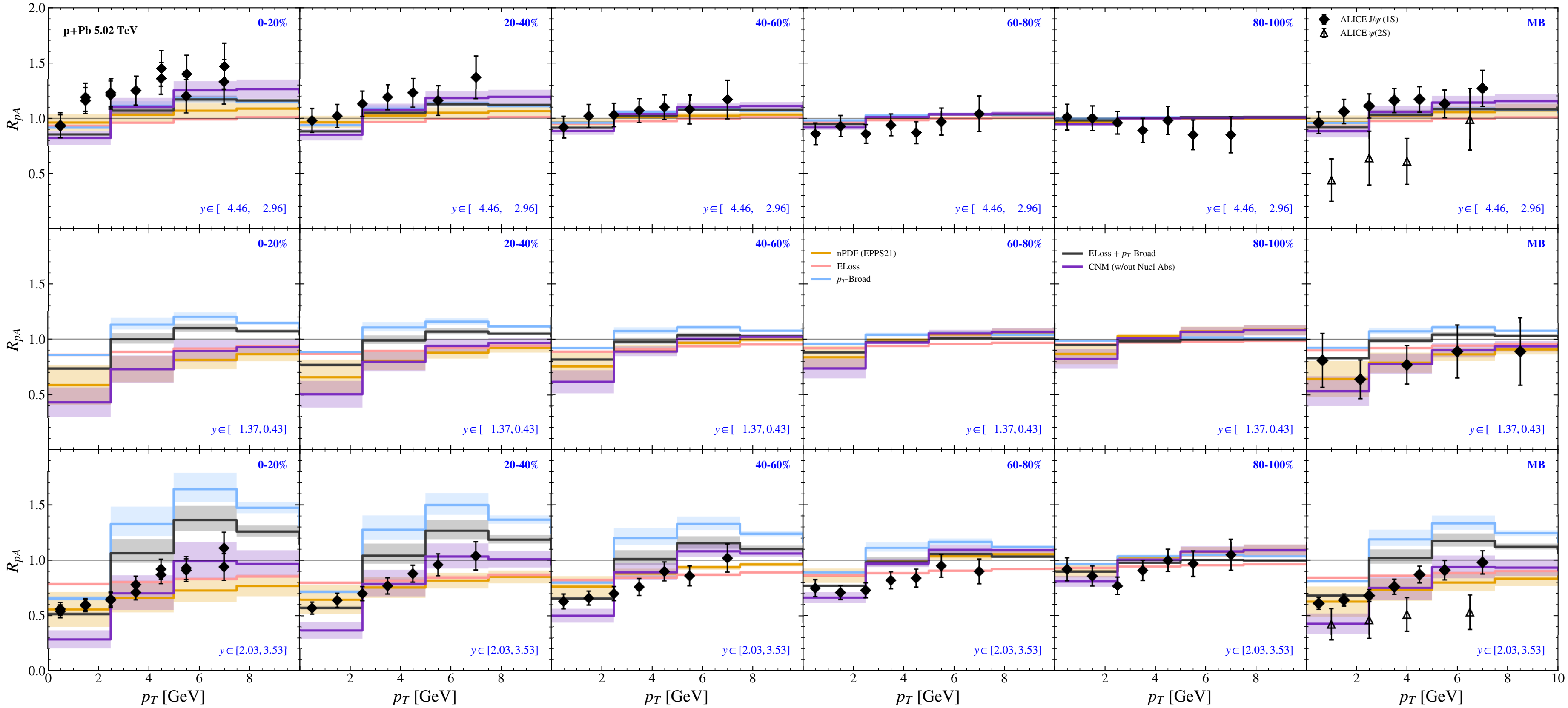

Using the EIC to Further Disentangle Cold and Hot Matter Effects

.

A Fixed-Target Program at the EIC

Conceptual notion of the EIC collision region with a fixed target

In the A-going direction (left) particle from fixed target $p + A$ and $A + A'$ collisions can be measured, top energy of $\sqrt{s_{NN}} \sim 14$ GeV for 100 GeV/nucleon Au beam

Cross sections for space radiation protection can also be measured

Either a gas jet target (like SMOG@LHCb) or target wires (like STAR BES II) can be used; likely target wires in ePIC

See the white paper, arXiv:2603.00265, and
workshop website https://indico.cfnssbu.physics.sunysb.edu/event/496/

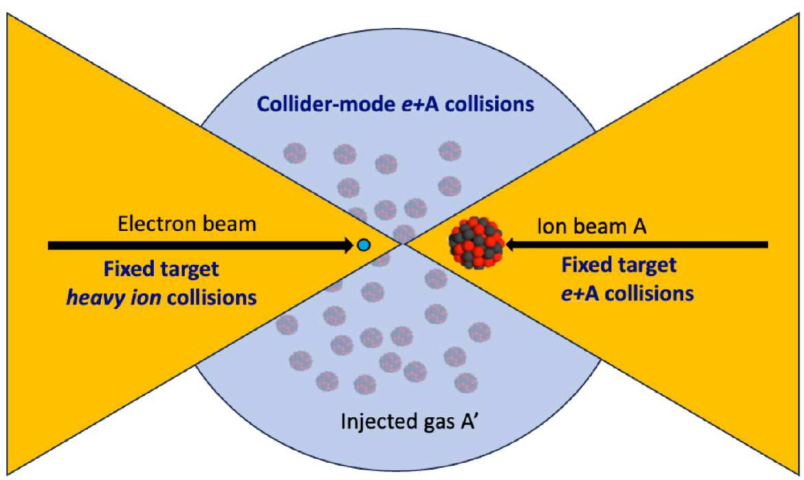

Challenges in Disentangling CNM Effects

Difficult to interpret multiple effects

Need to isolate specific effects through carefully chosen observables

Global approaches are important

Hot matter effects may play a role at collider energies

Cold QCD effects are a primary source of uncertainty in the interpretation of $A + A$ ***data***